

Supplementary Information

Rapid, room-temperature, solvent-free mechanochemical oxidation of elemental gold into organosoluble gold salts

*Jean-Louis Do,^{ab‡} Thomas Auvray,^{ac‡} Cameron B. Lennox,^{ac} Hatem M. Titi,^c Louis A. Cuccia,^b and
Tomislav Friščić^{ac*}*

a) School of Chemistry, University of Birmingham, Edgbaston, Birmingham, B15 2TT, United Kingdom

b) Department of Chemistry and Biochemistry, Concordia University, 7141 Sherbrooke Street West, H4B 1R6, Montreal, Canada

c) Department of Chemistry, McGill University, 801 Sherbrooke Street West, H3A 0B8, Montreal, Canada

**Corresponding author contact: t.friscic@bham.ac.uk*

1. Experimental Section

Material and methods: Unless otherwise specified, all reagents and solvents were purchased from commercial sources and used without further purification. The oxidation reactions of Au metal were carried out using a FTS1000 mill operating at a frequency of 30 Hz in 10 mL zirconia milling jar charged with a single zirconia ball (10 mm diameter, 3.4 g weight). The PXRD patterns were obtained in the 2θ range from 4° to 40° using a Bruker D2 PHASER X-Ray diffractometer equipped with a Cu- K_α ($\lambda = 1.54 \text{ \AA}$) source, LinxEye detector, and a Ni filter. FTIR-ATR spectra were obtained in the 400 cm^{-1} to 4000 cm^{-1} range on a Bruker Alpha 2 FTIR spectrometer equipped with an ATR module. ^1H NMR spectra were obtained on a Bruker AVIIIHD 500 spectrometer (500 MHz) with chemical shifts (δ) given in parts per million (ppm). High-resolution mass spectrometry data were collected on a Bruker Maxis QTOF. XPS Analysis was performed on a Fisher Scientific $K\alpha$ spectrometer using a spot size of $200 \mu\text{m}$, running 3 survey scans at 200 mV for 50 ms residence times and 10 scans for specific elements (similarly at residence times of 50 ms). Deconvolution and peak position were determined using Avantage software. Particle size analysis was conducted on toluene suspension equilibrated at 25°C using Dynamic Light Scattering (DLS) on a Brookhaven Instrument NanoBrook Omni analyser.

General procedure for the mechanochemical oxidation of elemental Au

Au metal (19.7 mg, 0.1 mmol) was added to a 10 mL zirconia jar charged with a single zirconia ball (10 mm diameter, 3.4 g). The desired halide source (**Table S1**) and Oxone® (94.0 mg, 0.3 mmol as KHSO_5) were added to the jar. The reaction mixture was then milled for 30 to 60 minutes. The resulting tetrahaloaurate salt were isolated by extraction using 2:1 v:v ratio of EtOAc:H₂O (see **Table S2** - a few drops of EtOH can be added to help with phase separation). The organic phase was dried on Na_2SO_4 and either freed of solvent under reduced pressure or left to slowly evaporate in air, leading to the formation overnight of crystals suitable for X-ray diffraction.

Table S1. Halide sources and amounts used in the mechanochemical oxidation of Au metal and resulting gold conversion (determined by gravimetric method after extraction)

Halide source	Amount (mmol)	Amount (mg)	Gold conversion %
TEACl	0.4	67.0	94 (± 2)
TBACl	0.4	113.0	89 (± 2)
TEABr	0.4	85.0	90 (± 3)
TBABr	0.4	131.0	94 (± 4)
CTABr	0.4	148.0	93 (± 2)
TEACl / KCl	0.11 / 0.3	17.0 / 23.0	88 (± 3)
TEABr / KBr	0.11 / 0.3	22.0 / 36.0	82 (± 3)
TBACl / KCl	0.11 / 0.3	30.0 / 22.0	89 (± 4)
TBABr / KBr	0.11 / 0.3	36.0 / 36.0	86 (± 6)
CTABr / KBr	0.11 / 0.3	40.0 / 36.0	84 (± 2)

Gravimetric determination of gold: After extraction, recrystallisation and drying in dessicator in the dark, the targeted tetrahaloaurate salt was suspended in aqueous methanol in a 9-dram vial and sonicated to give a homogenous solution or slightly cloudy suspension (in the case CTA[AuBr₄]). 3-4 mL of 5% aqueous hydroquinone solution was added to the solution/suspension and sonicated for 30 minutes and the mixture was subsequently heated in an 85°C oven for 30 minutes to ensure complete reduction to gold metal. After cooling, the precipitated gold was filtered onto a pre-weighed fiberglass filter paper disk, washed with water and methanol, dried in air, and the mass calculated by difference.

Table S2. Extraction efficiency^[a] using EtOAc in the presence and absence of H₂O.

Entry	Halide source	Gold recovery (%) ^[a]
1 ^[b]	TEACl (dried)	94 (±2)
2 ^[b]	TEABr (dried)	90 (±3)
3 ^[b]	TBACl	89 (±2)
4 ^[b]	TBABr	94 (±4)
5 ^[b]	CTABr	93 (±2)
6 ^[c]	TEACl	30 (±5)
7 ^[c]	TEABr	37 (±6)
8 ^[c]	TBACl	51 (±3)
9 ^[c]	TBABr	61 (±2)
10 ^[c]	CTABr	79 (±3)
11 ^[d]	TEACl	59 (±6)
12 ^[d]	TEABr	65 (±2)
13 ^[d]	TBACl	83 (±4)
14 ^[d]	TBABr	85 (±3)
15 ^[d]	CTABr	92 (±3)

[a] Conversion based on gravimetric determination of gold in, at least, two independent experiments conducted for 30 min; [b] Extraction performed using 2:1 v:v ratio of EtOAc:H₂O at room temperature; [c] Single-pass extraction performed using only EtOAc at room temperature; [d] Single-pass extraction performed using only EtOAc at 45°C.

TEA[AuCl₄], isolated as lime yellow crystalline plates by slow evaporation of an ethyl acetate solution.

¹H NMR (500 MHz, CDCl₃) δ 3.34 (q, J = 7.3 Hz, 8H), 1.44 – 1.39 (tt, 7.3, 1.8 Hz, 12H).

ESI-MS [M]⁻: Calc.: 338.8384, Found: 338.8406.

TEA[AuBr₄], isolated as orange-red crystalline plates by slow evaporation of an ethyl acetate solution.

¹H NMR (500 MHz, CDCl₃) δ 3.42 (q, J = 6.3 Hz, 8H), 1.44 – 1.39 (t, 6.3, 12H).

ESI-MS [M]⁻: Calc.: 516.6353, Found: 516.6347.

TBA[AuCl₄], isolated as lime yellow block by slow evaporation of an ethyl acetate solution.

¹H NMR (500 MHz, CDCl₃) δ 3.24 (m, 8H), 1.67 (m, 8H), 1.48 (m, 8H), 1.04 (t, J = 7.3 Hz, 12H).

ESI-MS [M]⁻: Calc.: 338.8384, Found: 338.8393.

TBA[AuBr₄], isolated as dark red block by slow evaporation of an ethyl acetate solution.

¹H NMR (500 MHz, CDCl₃) δ 3.28 (m, 8H), 1.70 (m, 8H), 1.50 (m, 8H), 1.05 (t, J = 7.3 Hz, 12H).

ESI-MS [M]⁻: Calc.: 516.6353, Found: 516.6343.

CTA[AuBr₄], isolated as dark red fine needles by slow evaporation of an ethyl acetate solution.

¹H NMR (500 MHz, CDCl₃) δ 3.33 (m, 2+9H), 1.74 (m, 2H), 1.36 (m, 4H), 1.26 (m, 22H), 0.88 (t, J = 7.3 Hz, 12H)

; ESI-MS [M]⁻: Calc.: 516.6353, Found: 516.6354.

One-pot two-step preparation of Au(I) salts from elemental gold

Gold metal (19.7 mg, 0.1 mmol) was added to a 10 mL zirconia jar charged with a single zirconia ball (10 mm diameter, 3.4 g). Oxone® (94.0 mg, 0.3 mmol as KHSO₅) was added to the jar and combined with either TBACl and KCl (30.0 and 22.0 mg, respectively) or TBABr and KBr (37.0 and 36.0 mg, respectively). The reaction mixture was then milled for 45 minutes. Anhydrous sodium acetylacetonate (15.0 mg, 1.1. eq) was added to the crude tetrahaloaurate salts (Cl: flashy yellow solid, Br: red solid) and the sample milled for 30 minutes. PXRD on the crude solid showed formation of the desired product. These were isolated by suspension in a 1:1 v:v ratio of Acetone:EtOH mix, filtration to remove insoluble and removal of the solvents under reduced pressure without external heat. The yellowish solids were recrystallised from absolute EtOH at 0 °C overnight, yielding colorless needles (75±4 % and 80±3 % for TBA[AuCl₂] and TBA[AuBr₂], respectively). Note: TBA[AuX₂] can be prepared using isolated

TBA[AuX₄] salts. This however usually results in higher degradation to elemental gold (purple by-product eliminated during work-up).

2. Powder X-Ray Diffraction (PXRD) Patterns

In the following figures, the simulated diffraction patterns are based on single crystal data (see below).

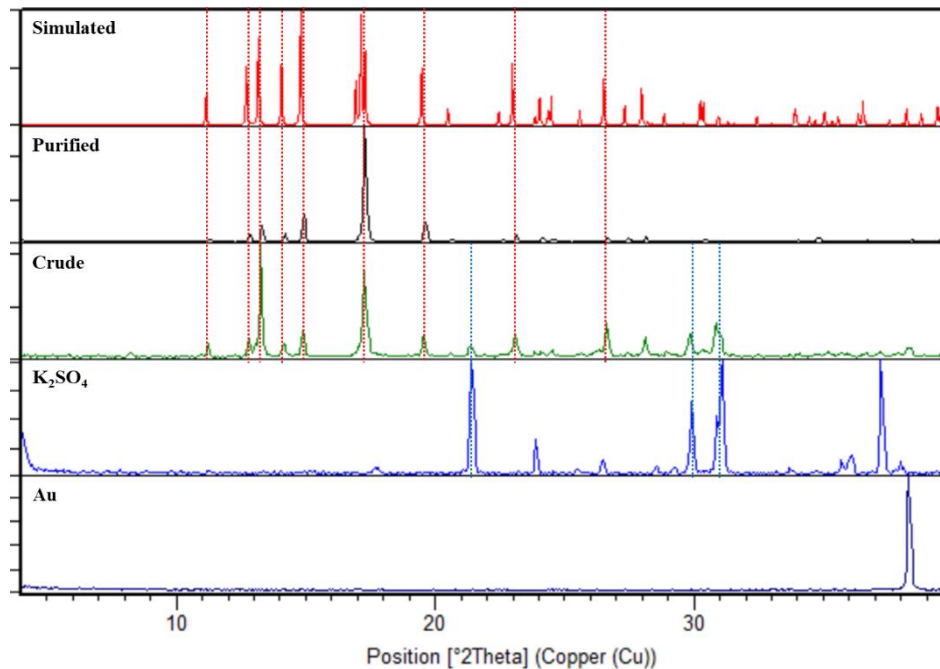


Figure S1. PXRD patterns for crude and purified reaction mixture of the oxidation of gold to **TEA[AuCl₄]** and selected reference patterns.

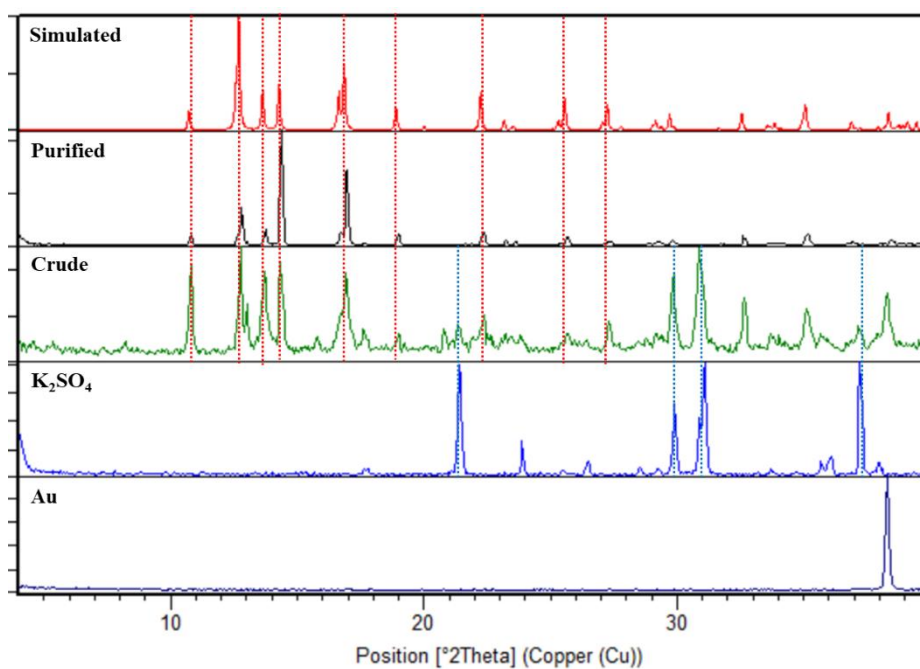


Figure S2. PXRD patterns for crude and purified reaction mixture of the oxidation of gold to **TEA[AuBr₄]** and selected reference patterns.

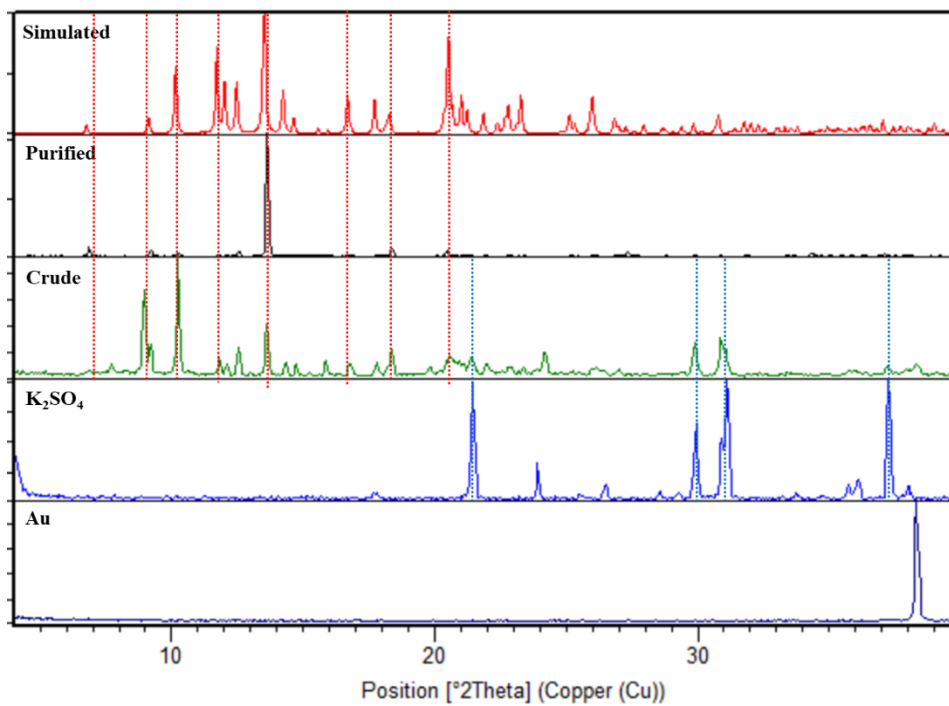


Figure S3. PXRD patterns for crude and purified reaction mixture of the oxidation of gold to **TBA[AuCl₄]** and selected reference patterns.

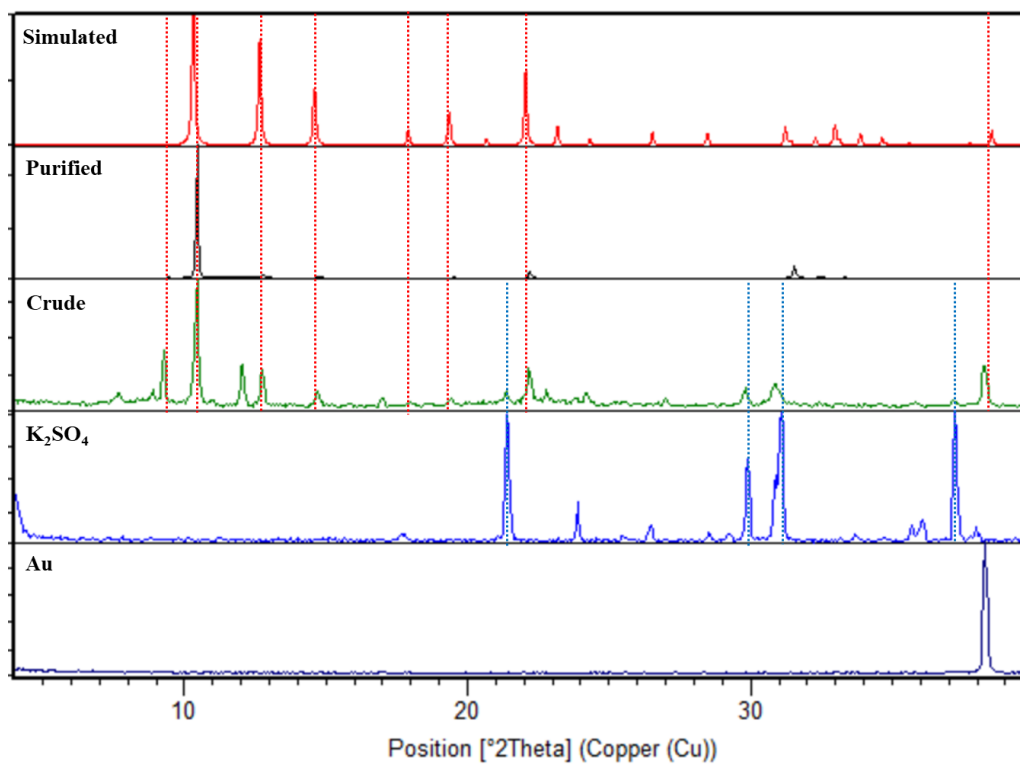


Figure S4. PXRD patterns for crude and purified reaction mixture of the oxidation of gold to **TBA[AuBr₄]** and selected reference patterns.

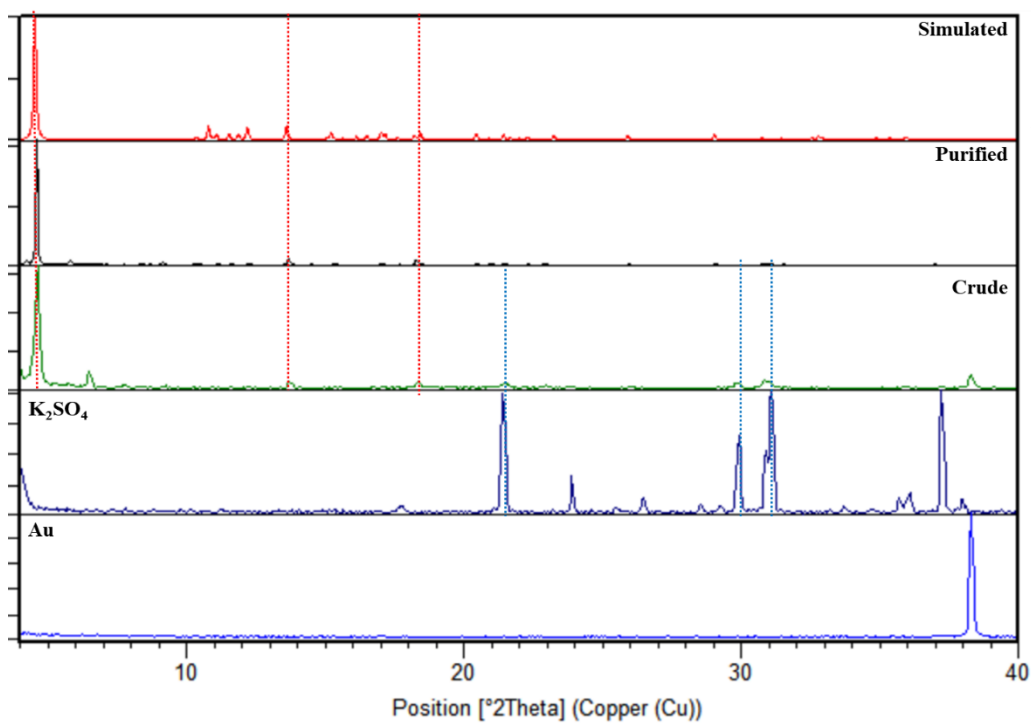


Figure S5. PXRD patterns for crude and purified reaction mixture of the oxidation of gold to **CTA[AuBr₄]** and selected reference patterns.

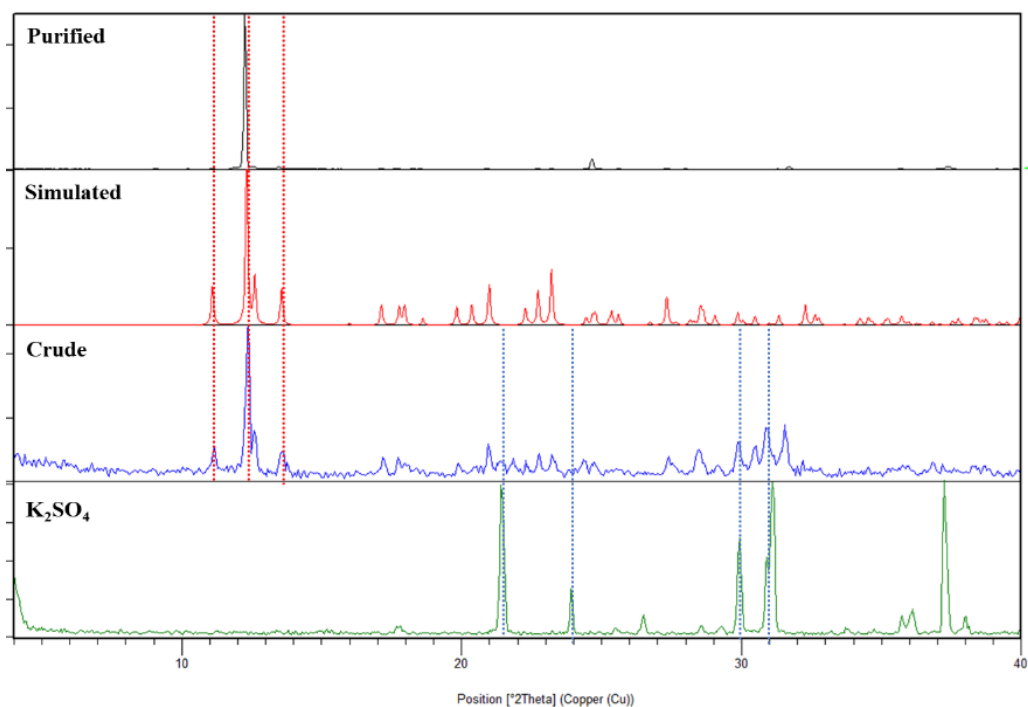


Figure S6. PXRD patterns for crude and purified reaction mixture of the two-steps one-pot preparation of $\text{CTA}[\text{AuCl}_2]$ and selected reference patterns.

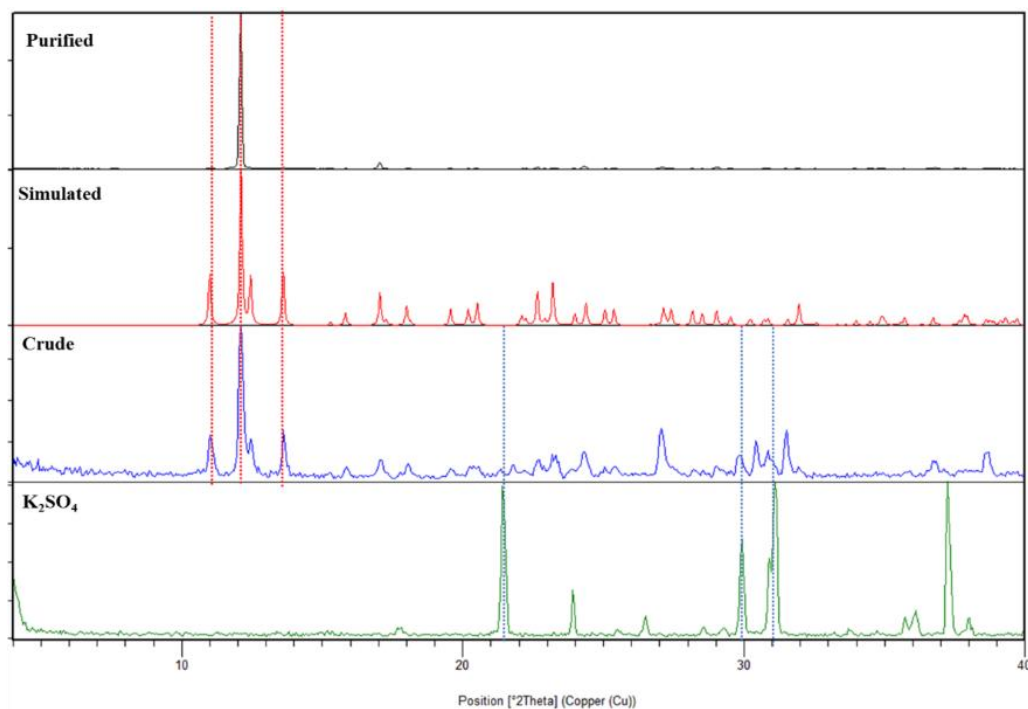


Figure S7. PXRD patterns for crude and purified reaction mixture of the two-steps one-pot preparation of $\text{CTA}[\text{AuBr}_2]$ and selected reference patterns.

3. ^1H NMR spectra

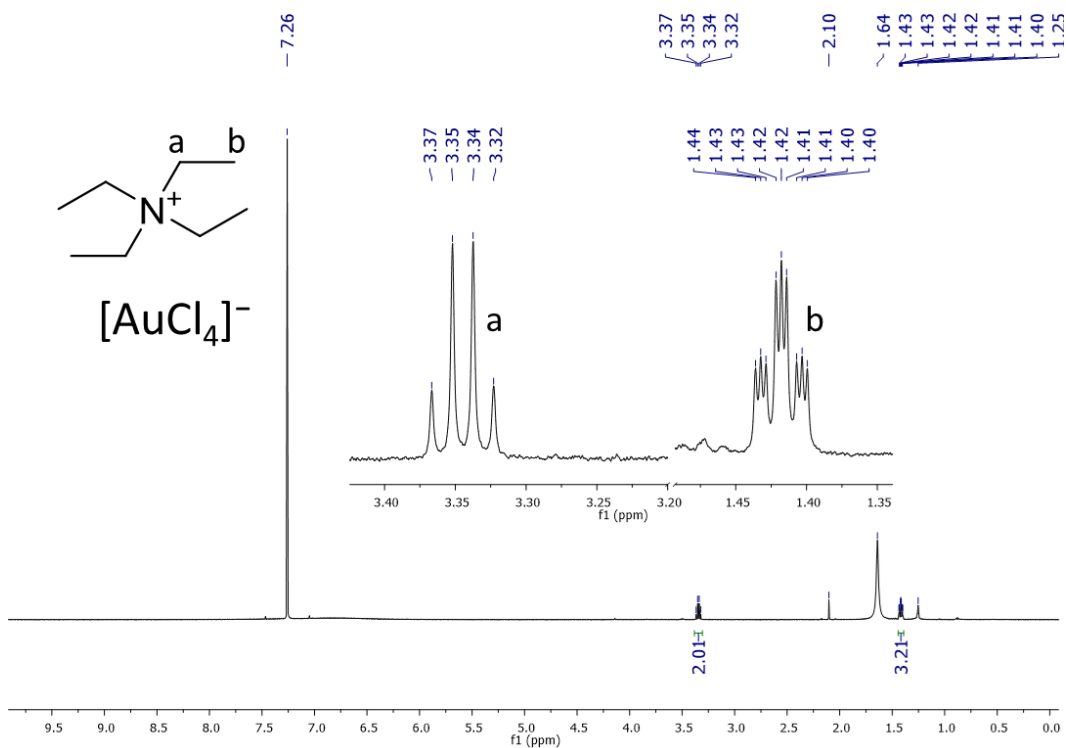


Figure S8. ^1H NMR of $\text{TEA}[\text{AuCl}_4]$ in CDCl_3

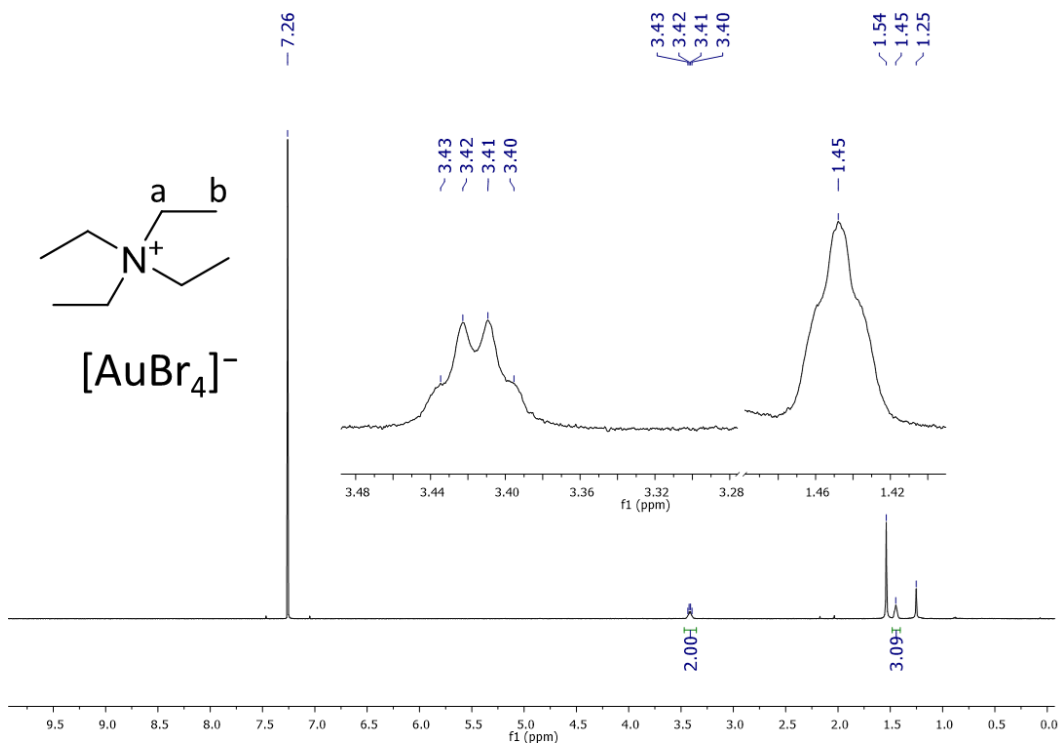


Figure S9. ^1H NMR of $\text{TEA}[\text{AuBr}_4]$ in CDCl_3

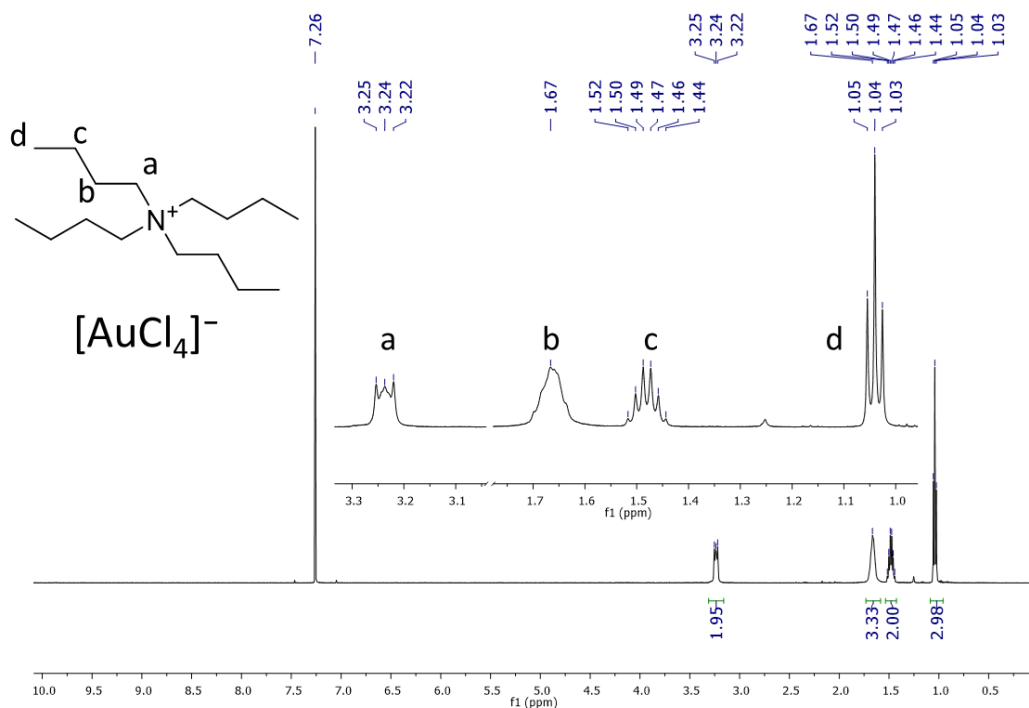


Figure S10. ^1H NMR of TBA $[\text{AuCl}_4]$ in CDCl_3

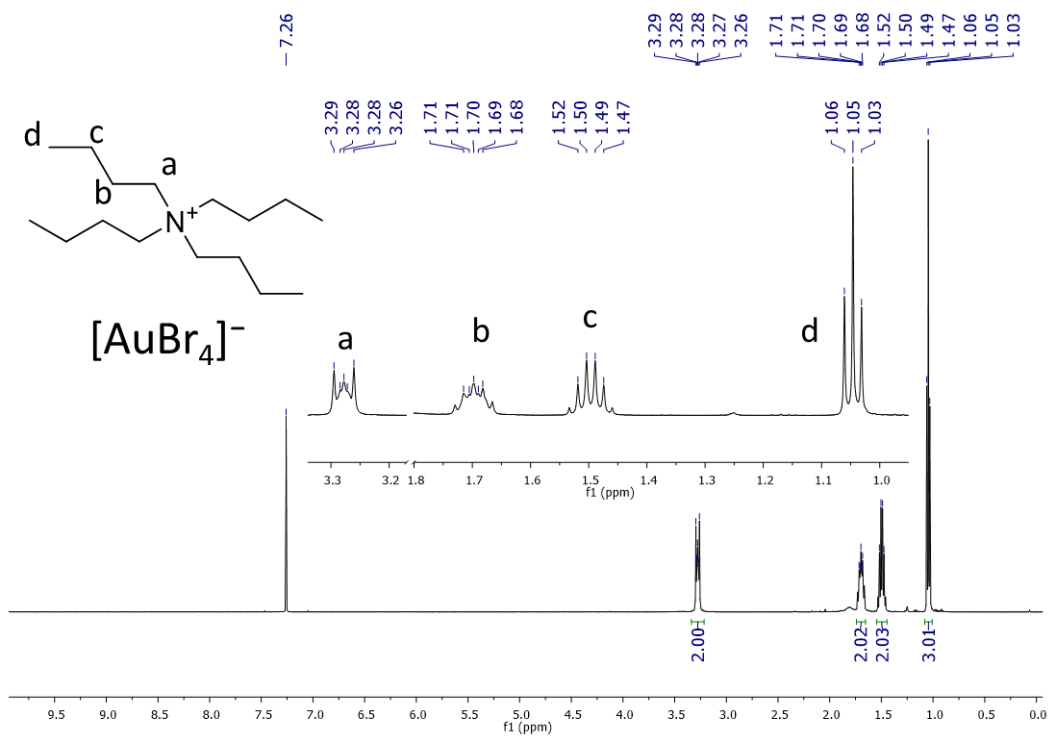


Figure S11. ^1H NMR of TBA $[\text{AuBr}_4]$ in CDCl_3

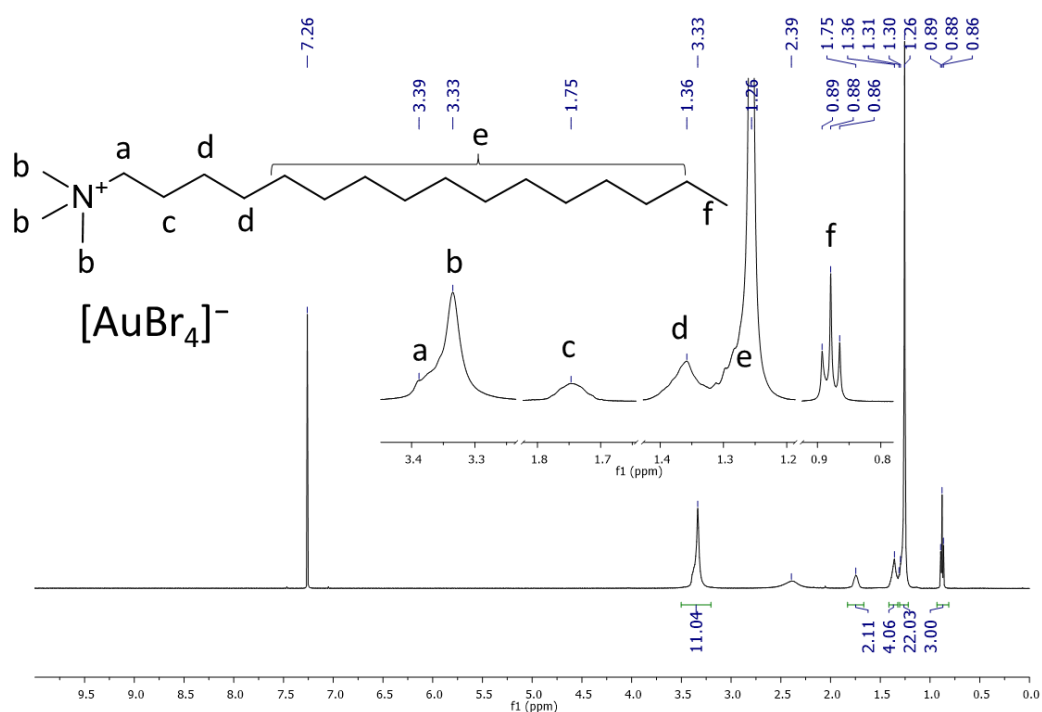


Figure S12. ^1H NMR of TEA[AuCl₄] in CDCl₃

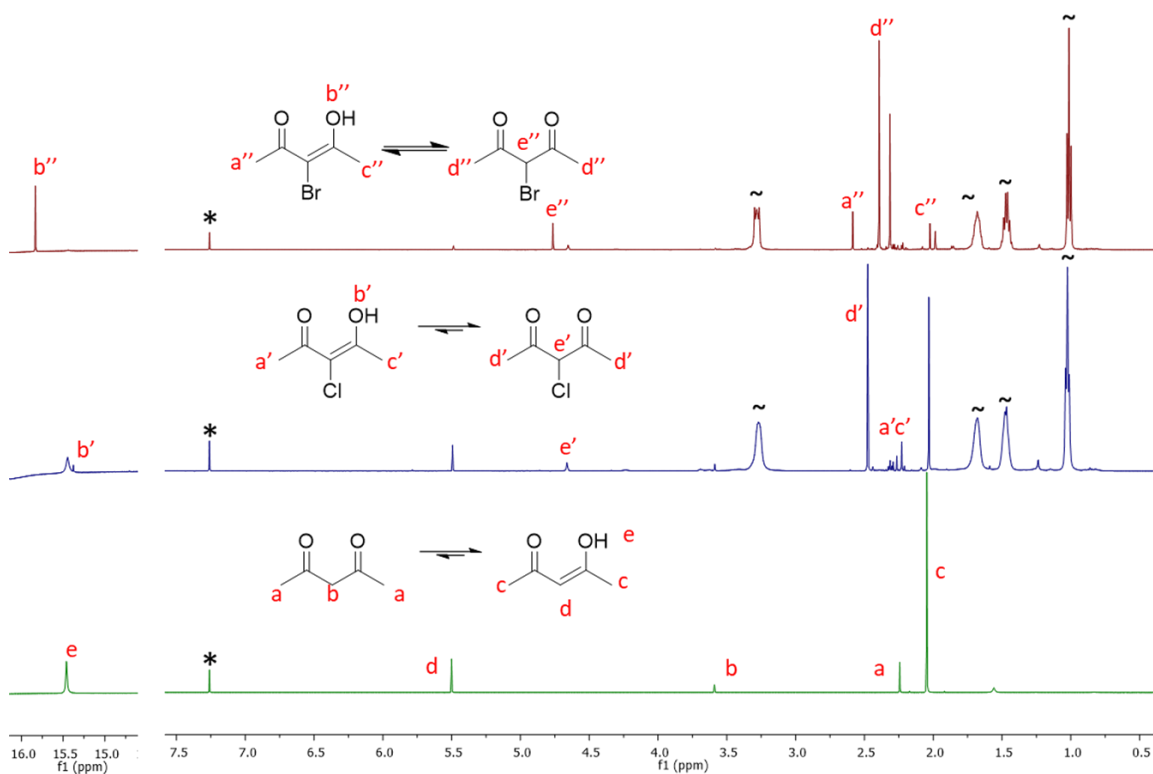


Figure S13. ^1H NMR of Hacac (bottom), the crude reaction mixture of TBA[AuCl₂] (middle) and the crude reaction mixture of TBA[AuBr₂] (top) in CDCl₃ (*). TBA resonances identified by ~. All three diketones presented the expected keto-enol equilibrium, which appeared affected by the presence of TBA salts in the crude mixtures (top and middle). Free Hacac was observed in all three spectra. Surprisingly, 3-Cl-acac is observed in the crude mixture of TBA[AuBr₂], presumably due to Cl-Br exchange in chloroform.

4. FT-IR spectra

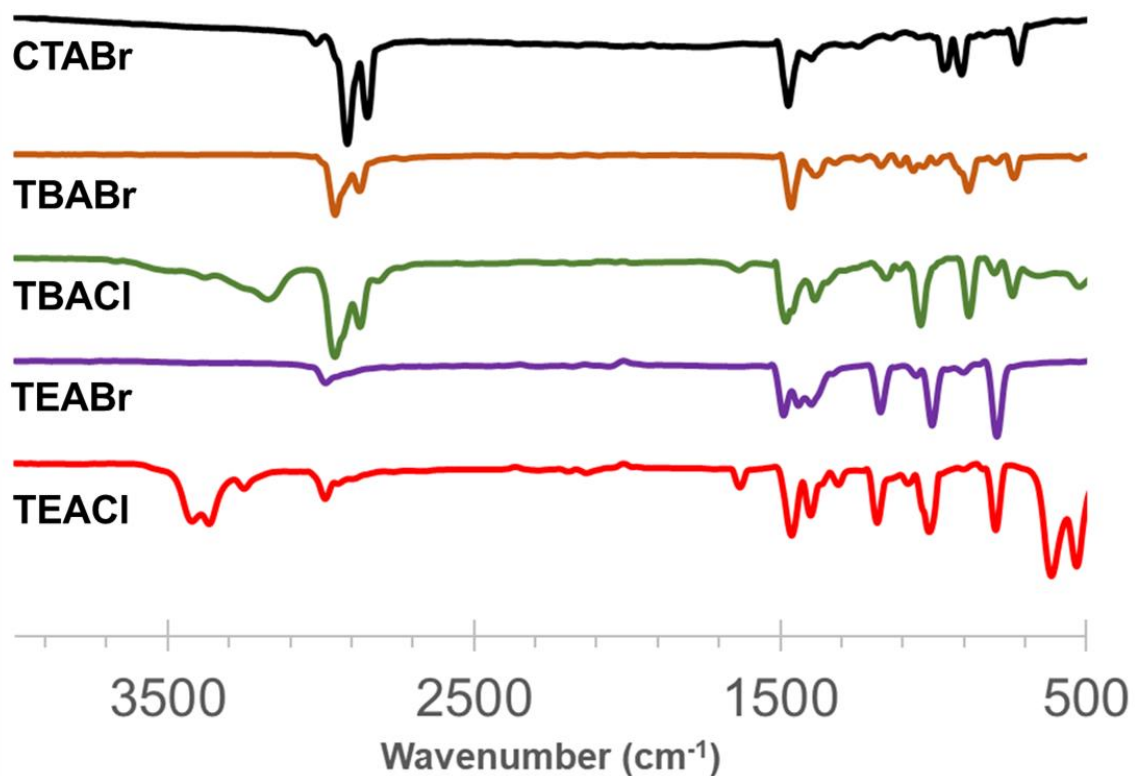


Figure S14. FT-IR spectra of the tetraalkylammonium halide salts

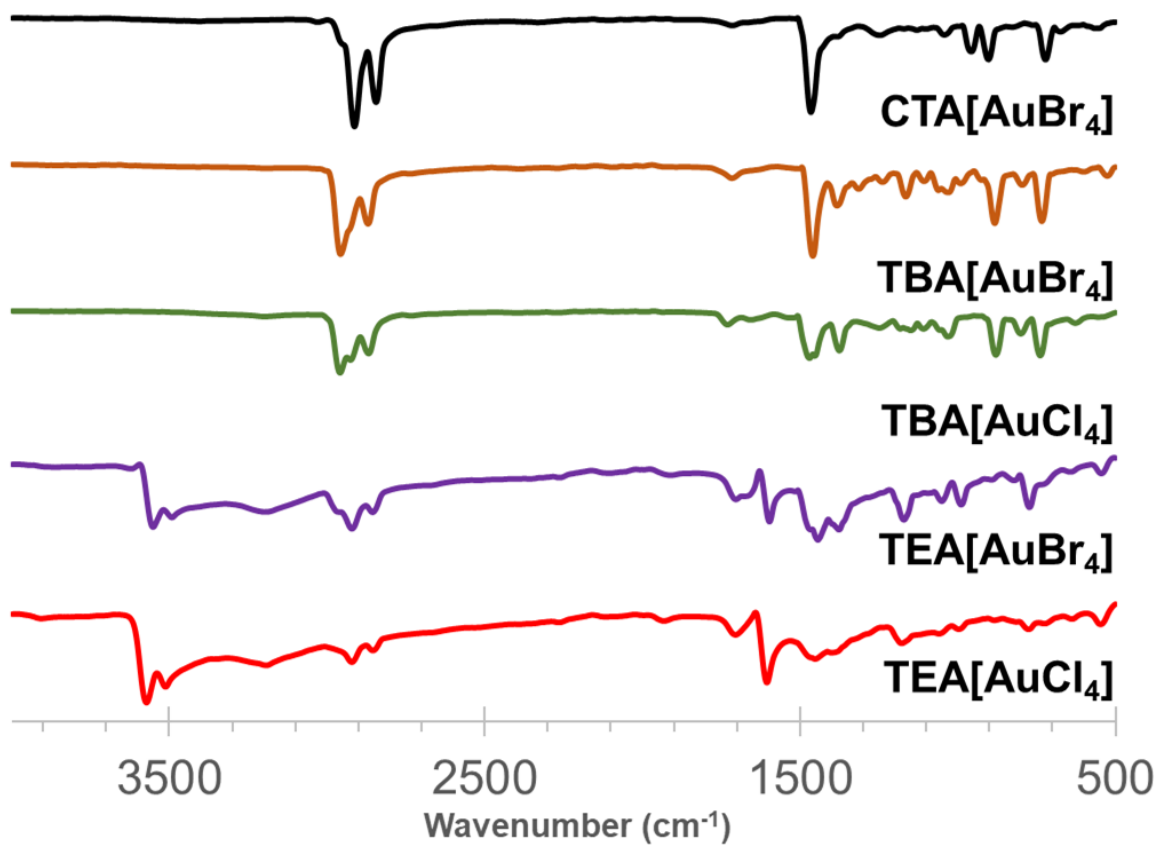


Figure S15. FT-IR spectra of the tetraalkylammonium tetrahaloaurate salts

5. XPS Analysis of crude milled samples – Au 4f region

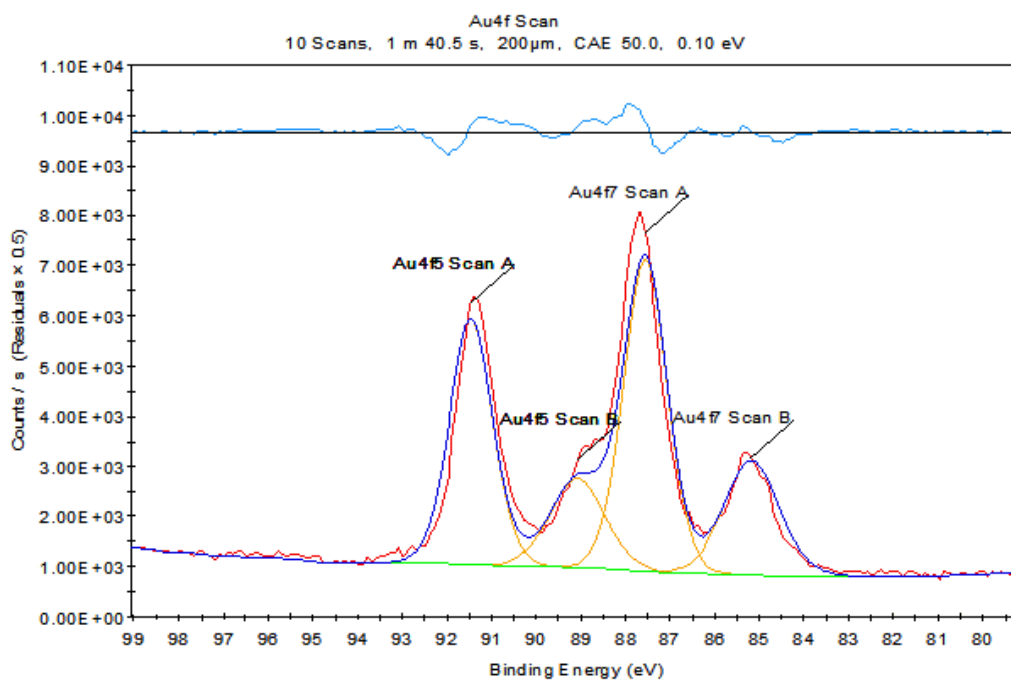


Figure S16. XPS spectrum of a crude **TEA[AuCl₄]** sample in the Au 4f region

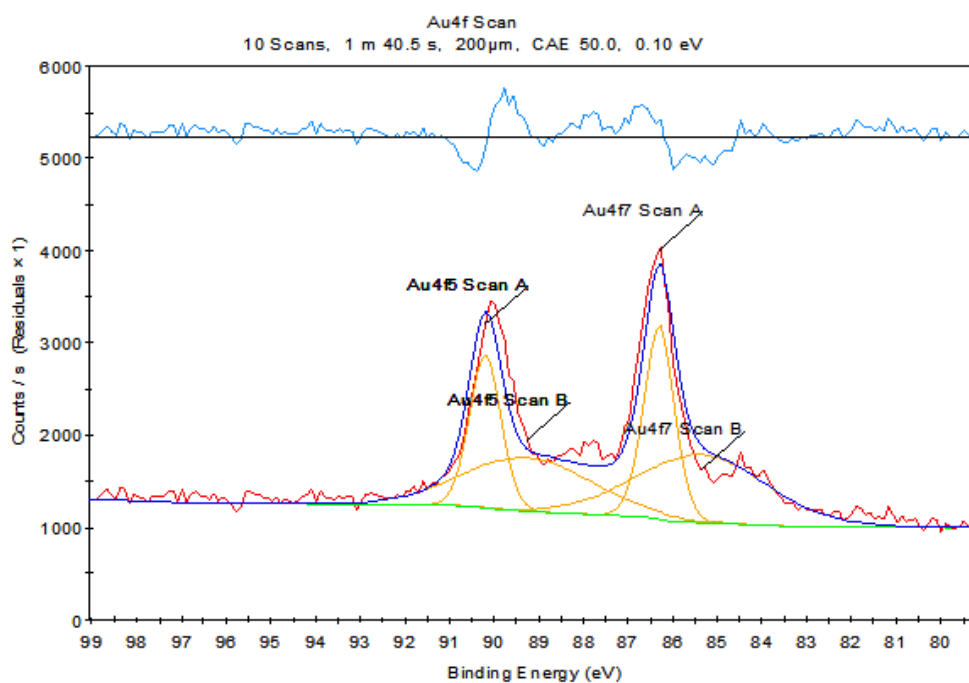


Figure S17. XPS spectrum of a crude **TEA[AuBr₄]** sample

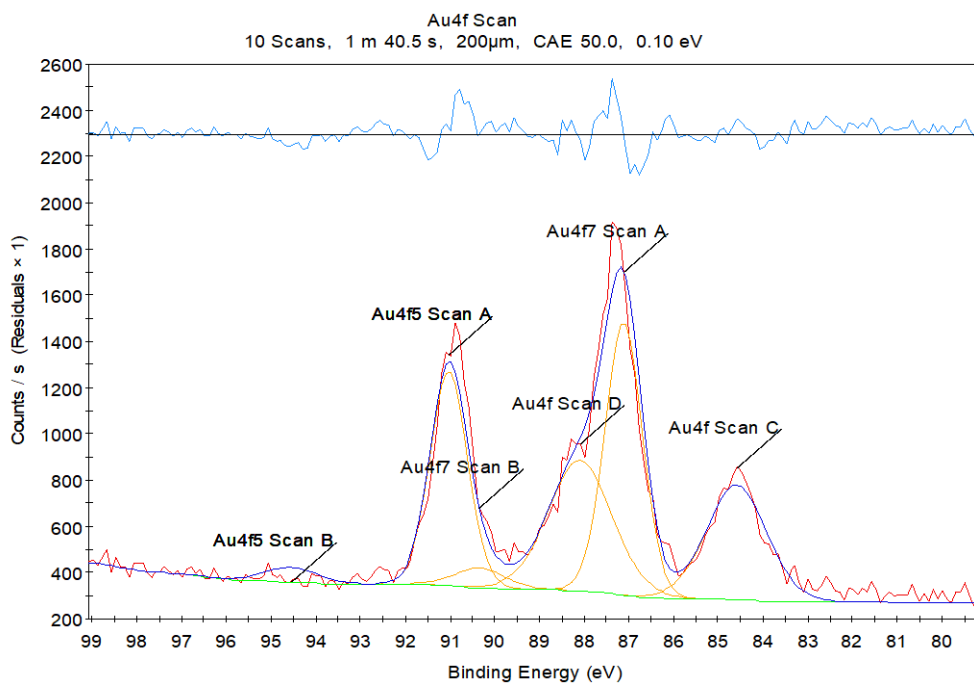


Figure S18. XPS spectrum of a crude **TBA[AuCl₄]** sample

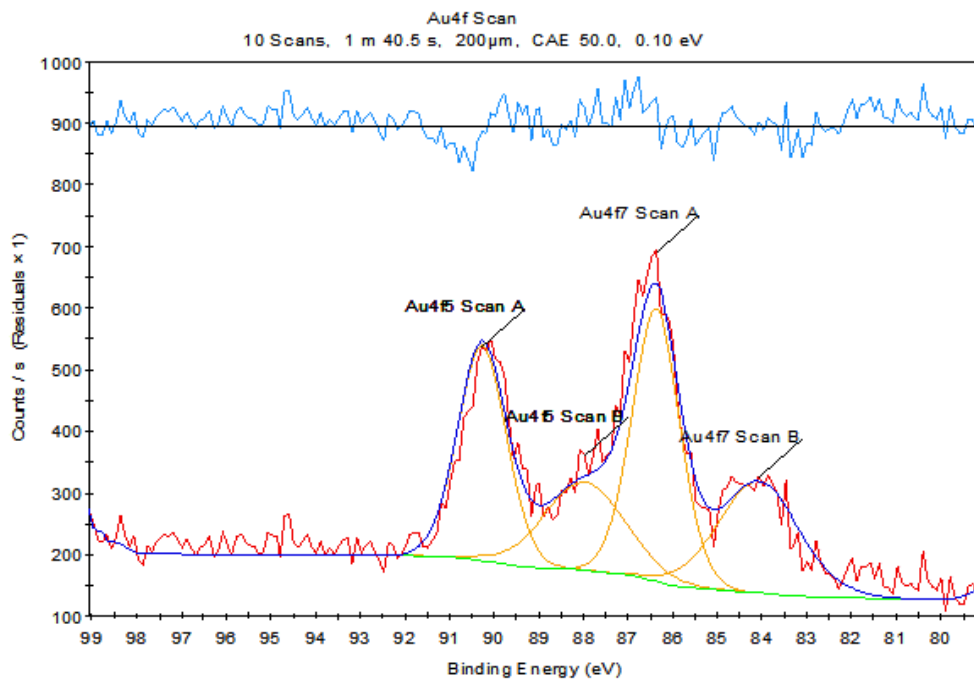


Figure S19. XPS spectrum of a crude **TBA[AuBr₄]** sample

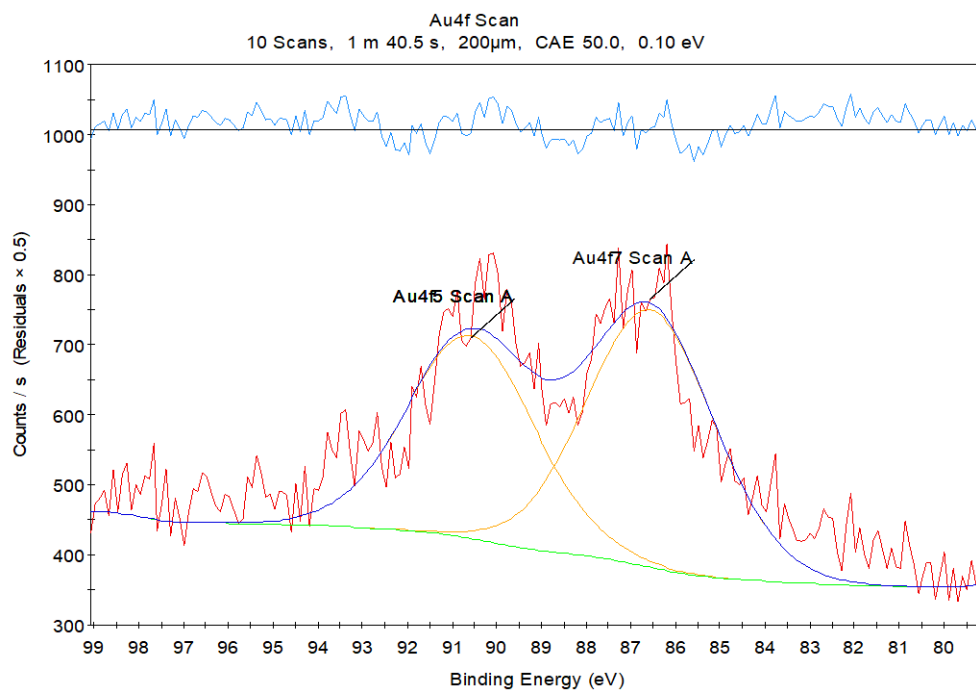


Figure S20. XPS spectrum of a crude **CTA[AuBr₄]** sample

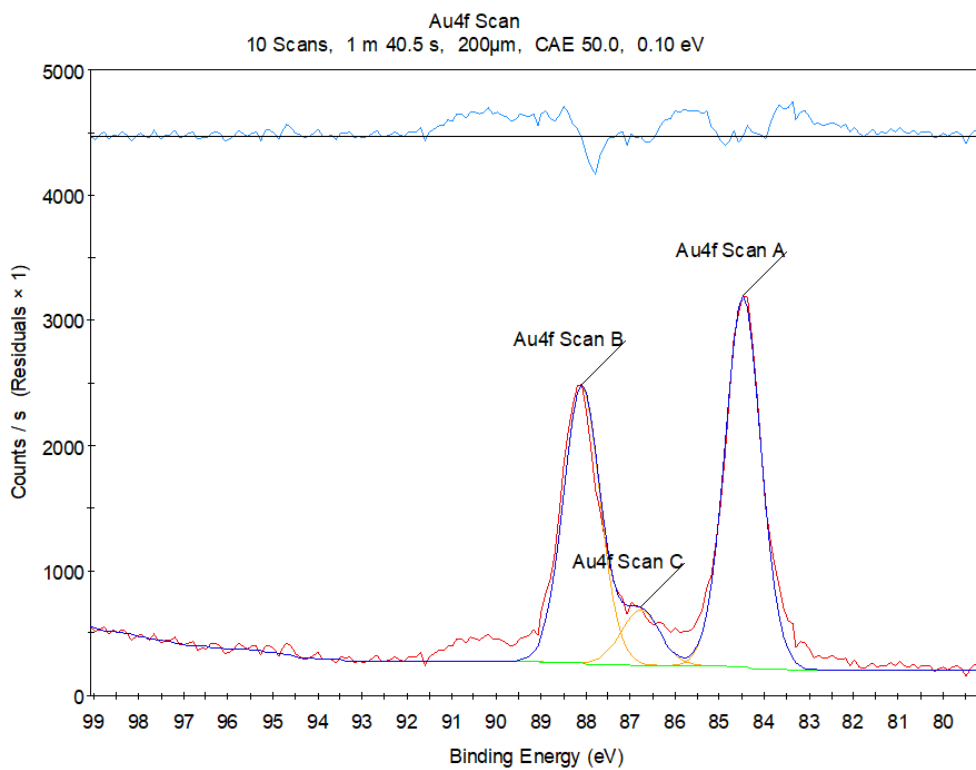


Figure S21. XPS spectrum of a crude **TBA[AuCl₂]** sample

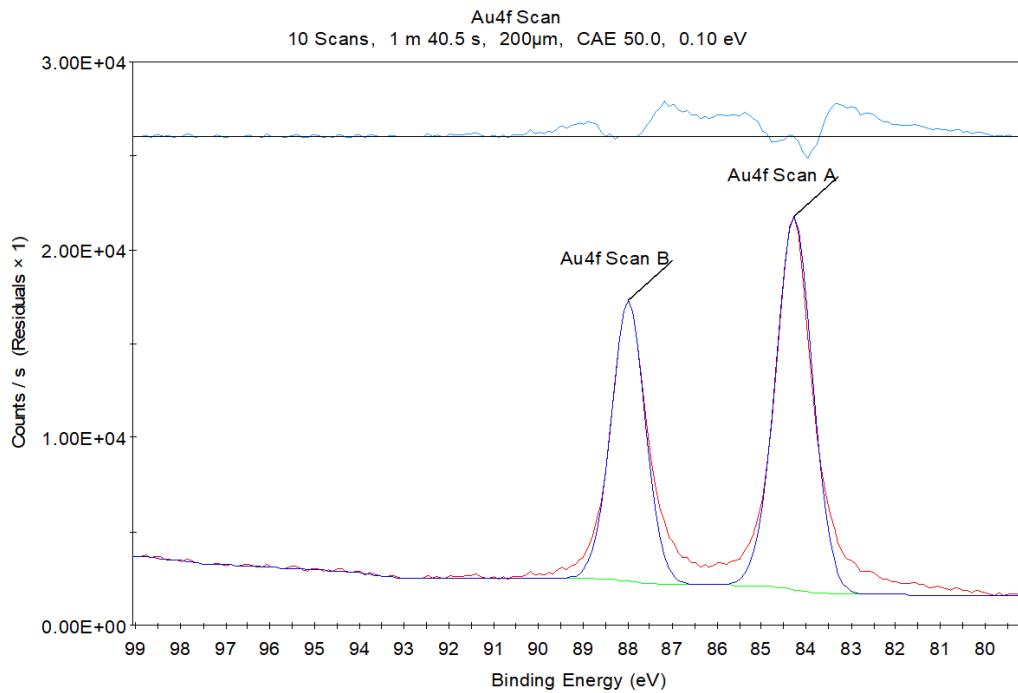


Figure S22. XPS spectrum of a crude **TBA[AuBr₂]** sample

6. Characterisation of mechanochemically prepared materials by determination of crystallographic unit cell dimensions after recrystallisation from ethyl acetate

Single crystal X-Ray diffraction data were measured on a Bruker D8 Venture diffractometer equipped with a Photon 200 area detector, and μ S microfocus X-ray source (Bruker AXS, $\text{CuK}\alpha$ source). All measurements were carried out at room temperature 298(2)K on crystal samples coated with a thin layer of amorphous paratone oil. Structure solution was carried out using the SHELXTL package in Olex2.^{1,2} The parameters were refined for all data by full-matrix-least-squares or F^2 using SHELXL.³ All of the non-hydrogen atoms were refined with anisotropic thermal parameters. Hydrogen atoms were placed in calculated positions and allowed to ride on the carrier atoms. All hydrogen atom thermal parameters were constrained to ride on the carrier atom.

Identification code	TEA[AuCl ₄]	TEA[AuBr ₄]	TBA[AuCl ₄]	TBA[AuBr ₄]	CTA[AuBr ₄]
CCDC deposition	2224725	2224727	2224728	2224729	2224730
Empirical formula	C ₈ H ₂₀ AuCl ₄ N	C ₈ H ₂₀ AuBr ₄ N	C ₁₆ H ₃₆ AuCl ₄ N	C ₁₆ H ₃₆ AuBr ₄ N	C ₁₉ H ₄₂ AuBr ₄ N
Formula weight	469.02	646.86	581.22	759.06	801.14
Temperature/K	298(2)				
Crystal system	monoclinic	monoclinic	monoclinic	tetragonal	monoclinic
Space group	<i>P2₁/n</i>	<i>P2₁/n</i>	<i>P2₁/n</i>	<i>P4/n</i>	<i>P2₁/c</i>
<i>a</i> /Å	9.1149(2)	9.3812(3)	14.8787(3)	12.1431(6)	8.1965(2)
<i>b</i> /Å	7.9249(2)	8.2418(3)	8.9310(2)	12.1431(6)	8.7398(2)
<i>c</i> /Å	10.3451(2)	10.5053(4)	18.2770(4)	8.5038(5)	38.9304(10)
α /°	90	90	90	90	90
β /°	92.0430(10)	90.562(2)	107.2590(10)	90	92.2710(10)
γ /°	90	90	90	90	90
Volume/Å ³	746.80(3)	812.21(5)	2319.32(9)	1253.93(14)	2786.62(12)
Z	2	2	4	2	4
$\rho_{\text{calc}}/\text{cm}^3$	2.086	2.645	1.665	2.010	1.910
μ/mm^{-1}	24.843	28.319	16.125	18.460	16.652
F(000)	444.0	588.0	1144.0	716.0	1528.0
Crystal size/mm ³	0.1 × 0.05 × 0.03	0.1 × 0.07 × 0.06	0.12 × 0.1 × 0.08	0.12 × 0.12 × 0.12	0.17 × 0.1 × 0.02
Radiation	CuK α ($\lambda = 1.54178$)				
2 θ range for data collection/°	20.512 to 144.872	16.572 to 144.938	6.756 to 145.014	14.66 to 144.948	9.094 to 144.774
Index ranges	-11 ≤ <i>h</i> ≤ 11 -9 ≤ <i>k</i> ≤ 9 -12 ≤ <i>l</i> ≤ 12	-11 ≤ <i>h</i> ≤ 11 -10 ≤ <i>k</i> ≤ 8 -12 ≤ <i>l</i> ≤ 12	-18 ≤ <i>h</i> ≤ 18 -11 ≤ <i>k</i> ≤ 11 -22 ≤ <i>l</i> ≤ 22	-15 ≤ <i>h</i> ≤ 15 -15 ≤ <i>k</i> ≤ 13 -10 ≤ <i>l</i> ≤ 10	-10 ≤ <i>h</i> ≤ 10 -9 ≤ <i>k</i> ≤ 10 -48 ≤ <i>l</i> ≤ 47
Reflections collected	8615	9295	23486	23881	52316
Independent reflections	1455 [R _{int} = 0.0399, R _{sigma} = 0.0276]	1592 [R _{int} = 0.0373, R _{sigma} = 0.0260]	4561 [R _{int} = 0.0641, R _{sigma} = 0.0461]	1238 [R _{int} = 0.0613, R _{sigma} = 0.0281]	5462 [R _{int} = 0.0847, R _{sigma} = 0.0433]
Data/restraints/parameters	1455/0/68	1592/0/68	4561/0/204	1238/47/80	5462/162/225
Goodness-of-fit on F ²	1.116	1.043	1.051	1.168	1.082
Final R indexes [I >= 2 σ (I)]	R ₁ = 0.0188, wR ₂ = 0.0440	R ₁ = 0.0280, wR ₂ = 0.0698	R ₁ = 0.0568, wR ₂ = 0.1422	R ₁ = 0.0759, wR ₂ = 0.1804	R ₁ = 0.0762, wR ₂ = 0.2057
Final R indexes [all data]	R ₁ = 0.0198, wR ₂ = 0.0445	R ₁ = 0.0301, wR ₂ = 0.0720	R ₁ = 0.0684, wR ₂ = 0.1604	R ₁ = 0.0819, wR ₂ = 0.1886	R ₁ = 0.1000, wR ₂ = 0.2260
Largest diff. peak/hole / e Å ⁻³	0.59/-0.70	0.87/-0.99	1.61/-1.86	1.74/-0.95	2.18/-1.63

TEA[AuCl₄]: The asymmetric unit contains only half molecules : three chlorides connected to the gold centre were identified in the asymmetric unit cell, with partial occupancy of 50% for two of them.

TEA[AuBr₄]: The tetraethylammonium salts are isostructural. The asymmetric unit contains only half molecules. Three bromides connected to the gold centre were identified in the asymmetric unit cell, with partial occupancy of 50% for two of them.

TBA[AuBr₄]: Both ions sit on fourfold axis, passing through the gold and nitrogen atoms, respectively. The n-butyl chain appeared disordered and two overlapping orientations were modelled using appropriate restraints.

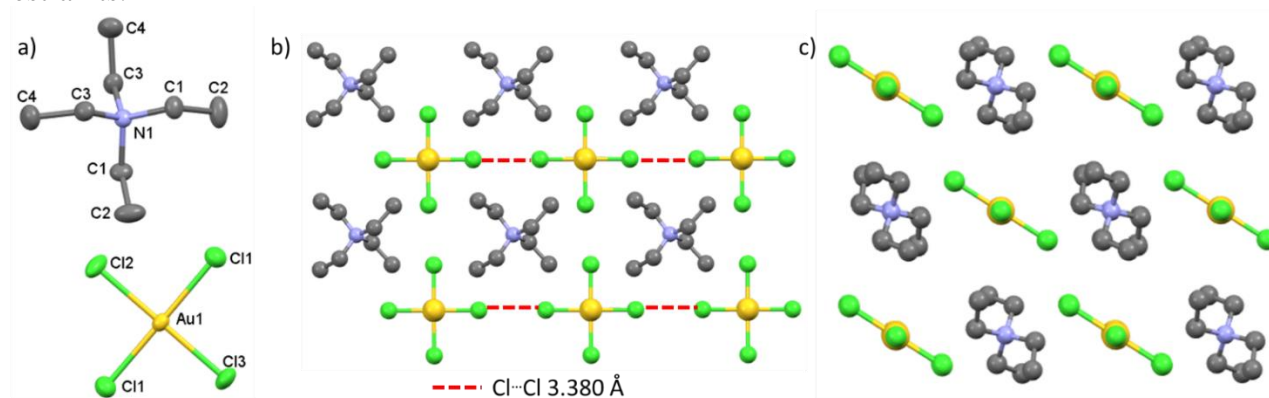


Figure S23. A) Ellipsoid (30% probability) representation of TEA[AuCl₄], B) crystal packing along the *a*-axis, highlighting close Cl-Cl contacts and C) along the *b*-axis.

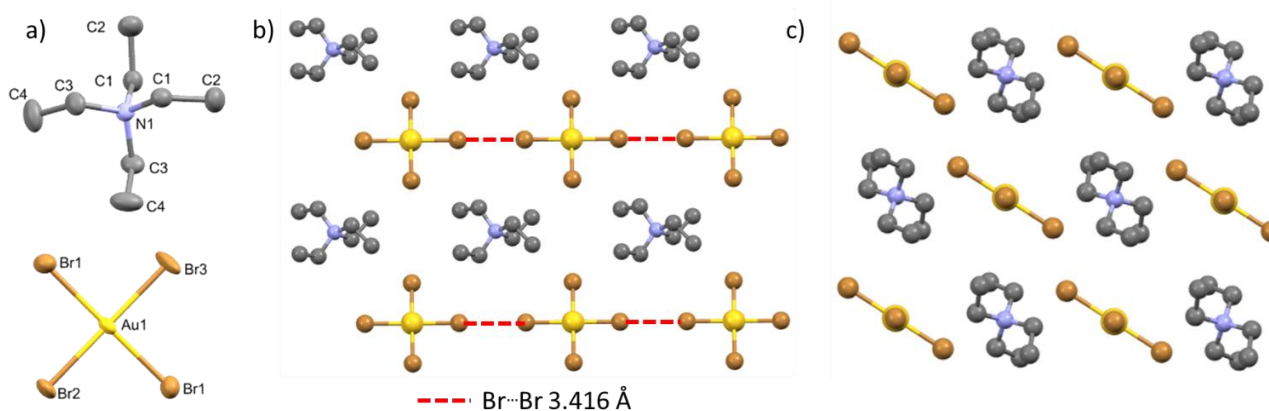


Figure S24. A) Ellipsoid (30% probability) representation of TEA[AuBr₄], B) crystal packing along the *a*-axis, highlighting close Br-Br contacts and C) along the *b*-axis.

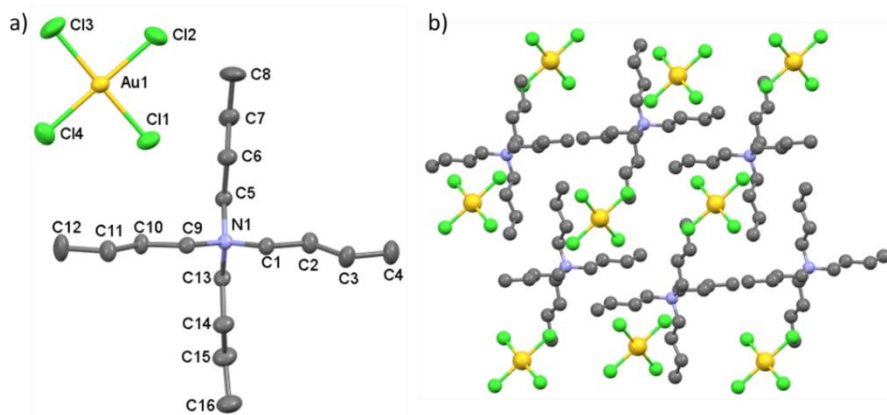


Figure S25. A) Ellipsoid (30% probability) representation of TBA[AuCl₄] and B) the crystal packing along the *b*-axis.

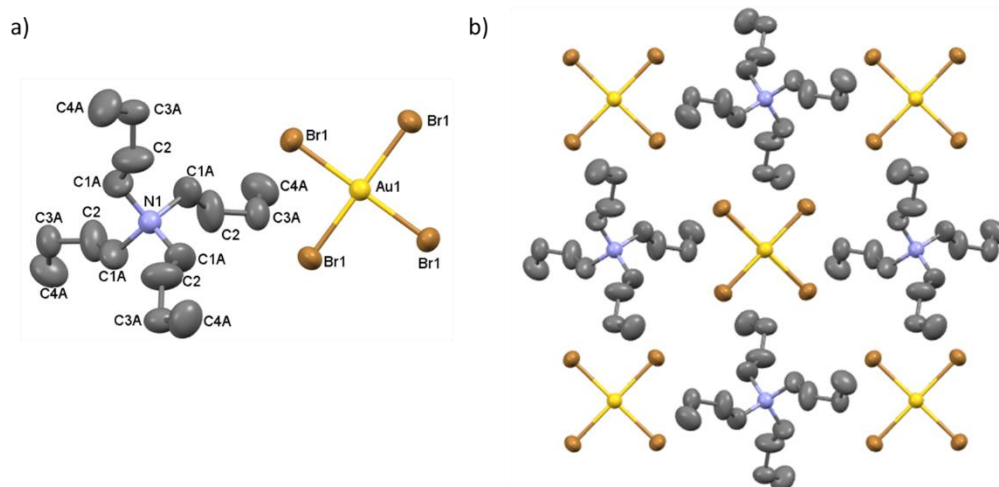


Figure S26. A) Ellipsoid (30% probability) representation of TBA[AuBr₄] (only one of the two part shown for the disorder n-butyl chain) and B) the crystal packing along the *c*-axis.

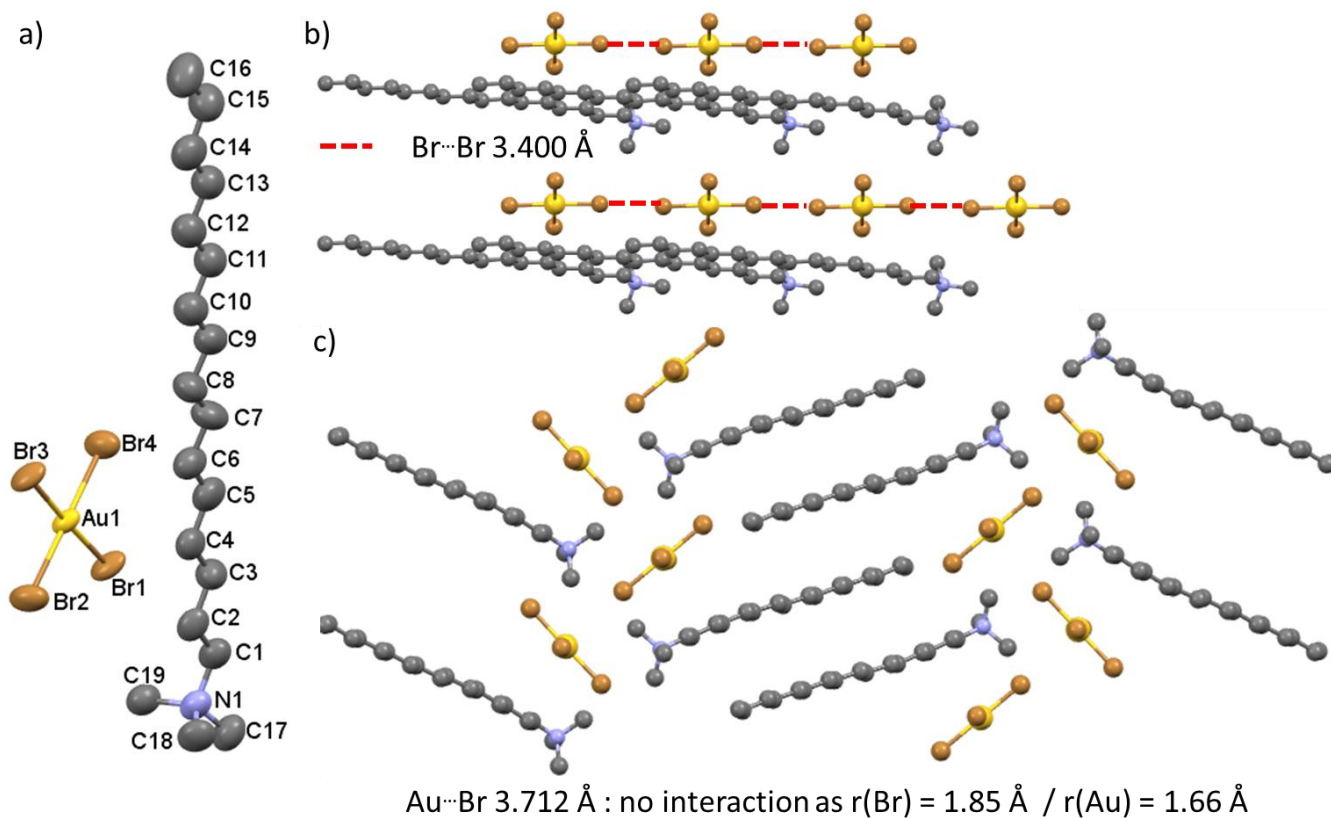


Figure S27. A) Ellipsoid (30% probability) representation of CTA[AuBr₄] and the crystal packing along B) the *b*-axis, highlighting close Br-Br contacts and C) the *a*-axis.

7. DLS analysis

A toluene suspension of CTA⁺ stabilised gold nanoparticles was equilibrated at 25 °C and size analysis was conducted in quadruplicate.

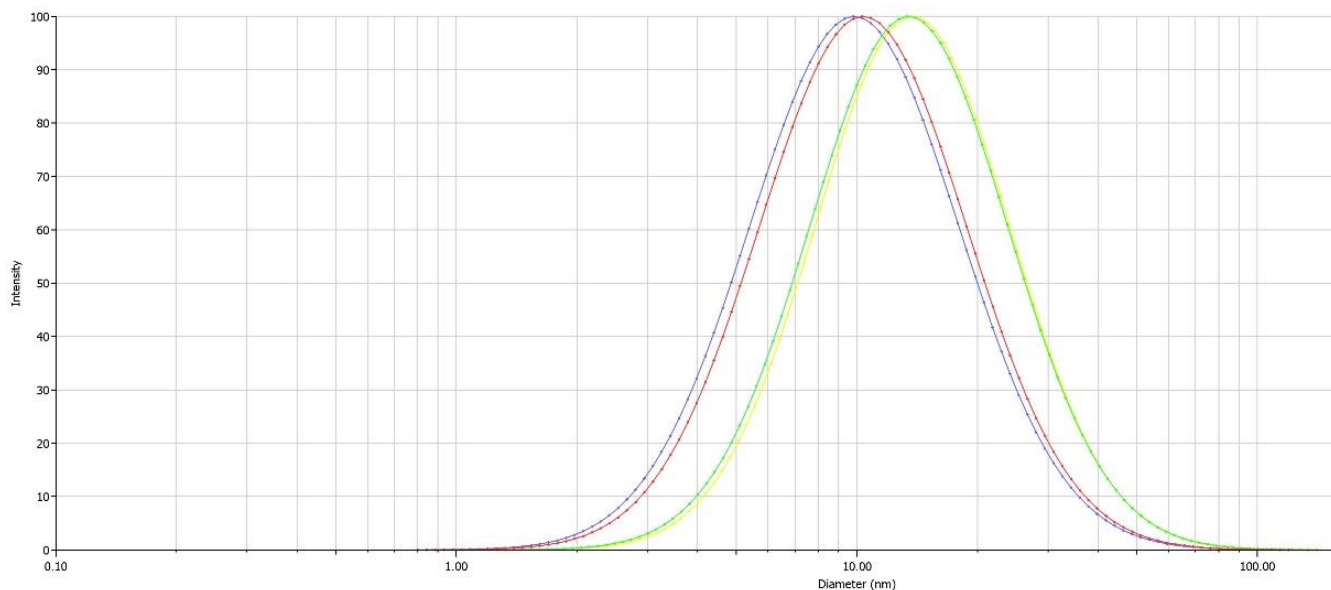


Figure S28. Logarithmic distribution of the nanoparticles size in a toluene suspension of Au NPs prepared using CTA[AuBr₄] and NaBH₄.

Type	Sample ID	Eff. Diam. (nm)	Polydispersity	Count Rate (kcps)
DLS	CTAAU _{Br} 4 Au NPs - 1	10.36	0.425	109.7
DLS	CTAAU _{Br} 4 Au NPs - 2	13.47	0.383	110.2
DLS	CTAAU _{Br} 4 Au NPs - 3	9.85	0.436	107.7
DLS	CTAAU _{Br} 4 Au NPs - 4	13.75	0.368	108.0
	Mean:	11.86	0.403	108.9
	Std Err:	1.02	0.016	0.6
	Std Dev:	2.04	0.033	1.2

8. Control Experiments

Table S3. Oxidation of gold in aqueous heterogeneous suspension^[a-b]

Entry	Form of gold	Gold conversion %
1	20 mesh	10-15
2	6 mm shot	trace
3	1.4 mm diameter wire	≤ 5
4	0.5 mm diameter wire ^[c]	≤ 5

[a] All aqueous suspension experiments were conducted using 0.1 mmol of Au, 0.4 mmol KCl, and 0.3 mmol Oxone® in 10 mL of distilled H₂O in a silanised 6 dram vial equipped with a 4.5 mm diameter magnetic stir bar, stirred at 600 RPM for 30 minutes; [b] All experiments were compared to mechanochemical experiments utilizing the same forms of Au, reaction times, and ratio of reagents. The conversions under mechanochemical conditions were in all cases ≥ 90%; [c] 93:7 Au: Pd alloyed wire

Table S4. Oxidation of gold under mechanical stirring^[a-c]

Entry	Form of gold	Gold conversion %
1 ^[d]	20 mesh	N/A ^[g]
2 ^[d]	6 mm shot	trace
3 ^[d]	1.4 mm diameter wire	trace
4 ^[d]	0.5 mm diameter wire ^[f]	trace
5 ^[e]	20 mesh	N/A ^[g]
6 ^[e]	6 mm shot	trace
7 ^[e]	1.4 mm diameter wire	trace
8 ^[e]	0.5 mm diameter wire ^[f]	trace

[a] All mechanical stirring experiments were conducted using solid reagents, 0.1 mmol of Au, 0.4 mmol KCl, and 0.3 mmol Oxone® in a silanised 6 dram vial equipped with a 4.5 mm diameter magnetic stir bar; [b] KCl and Oxone® were individually milled in a Retsch MM400 at 29.5Hz for 5 minutes into fine powders to enable sieving and separation of the Au from the remaining reagents; [c] All experiments were compared to mechanochemical experiments utilizing the same forms of Au, reaction times, and ratio of reagents. The conversions under mechanochemical conditions were in all cases $\geq 90\%$; [d] Experiment conducted at 600 RPM for 30 minutes; [e] Experiment conducted at 900 RPM for 30 minutes [f] 93:7 Au:Pd alloyed wire; [g] Au powder too fine to separate from other reagents using a sieve for gravimetric determination of gold conversion.

9. References

1. G.M. Sheldrick, SHELXT - Integrated space-group and crystal-structure determination, *Acta Cryst.* **2015**, A71, 3-8
2. O. V. Dolomanov, L. J. Bourhis, R. J. Gildea, J. A. K. Howard and H. Puschmann. "OLEX2: a complete structure solution, refinement and analysis program". *J. Appl. Cryst.* **2009**, 42, 339- 341
3. G.M. Sheldrick, Crystal structure refinement with SHELXL, *Acta Cryst.* **2015**, A71, 3-8